

The Effect of Damage Nucleation on the Toughness of an Adhesive Joint

M. N. CAVALLI^a and M. D. THOULESS^{a, b, *}

^a*Department of Mechanical Engineering;* ^b*Department of Materials Science
and Engineering, University of Michigan, Ann Arbor, MI 48109, USA*

(Received 9 September 2000; In final form 22 November 2000)

The intrinsic toughness of an adhesive joint has been shown to be different depending on whether the adherends remain elastic or deform in a plastic fashion. This phenomenon occurs because the different constraint imposed by the adherends results in a change in the deformation mechanisms of the adhesive layer. In the elastic geometry, damage nucleation occurs when the stresses in the adhesive layer reach a critical value before the conditions for fracture are met. Void growth then leads to large-scale bridging across the adhesive layer and an increase in the measured toughness. In contrast to this behavior, the reduced constraint associated with adherends that are thin enough to deform plastically allows the fracture criterion to be met before damage nucleation occurs. There is then no bridging contribution to the toughness. The effect of damage in an adhesive layer can be viewed either as a bridging zone behind the crack tip, or as an extended cohesive zone ahead of the crack tip. The toughness of an adhesive joint can either be increased or decreased by the nucleation of damage. The effects of a damage zone on the behavior of an adhesive joint with elastic adherends are discussed, and it is shown how numerical techniques can be used to model this behavior and to deduce the fracture parameters.

Keywords:

1. INTRODUCTION

The advantages of adhesive bonding over traditional joining techniques have been well-documented. They include a larger range of materials that can be joined, stiffer joints resulting in lighter

*Corresponding author. Tel.: 734-647-3170, Fax: 734-763-5289, e-mail: thouless@engin.umich.edu

construction [1], reduced stress concentrations, increased fatigue resistance [2], and an increase in corrosion resistance [1]. These gains depend on the ability of a designer to predict the overall strength and reliability of the bond. Over the past thirty years, much work has been done to use the concepts of linear-elastic fracture mechanics (LEFM) to characterize both the strength and toughness of adhesive joints [2–4]. More recently, various researchers have provided analyses of joints in which the requirements for LEFM are violated [5–9]. It is clear that understanding the behavior of adhesive joints under both sets of conditions is essential to realize the potential of adhesive joining.

To ensure the validity of tests conducted under LEFM conditions, there must be no significant non-linear deformation before crack growth occurs. Provided this condition is met, it is possible to deduce a value of toughness from the load and deflection behavior for a particular adhesive joint that is independent of the geometry of the joint [2]. Two geometries that are often used for mode-I (pure opening) loading are the double-cantilever beam (DCB) and a variant, the tapered double-cantilever beam (TDCB) [10]. Both configurations provide similar information, but the latter has the advantage of providing an approximately constant rate of change of compliance with respect to crack length.

Thin adherends, such as sheet metal, bonded with a tough adhesive are sometimes subjected to sufficiently large loads and bending moments to cause plastic deformation of the metal before the adhesive fails. LEFM criteria are not valid under these conditions, and the geometry cannot be analyzed within this framework. When gross plastic deformation of the adherends occurs, it is necessary to use numerical approaches to evaluate the toughness. This has been demonstrated by Yang *et al.* [7–9], using the cohesive-zone approach of Needleman [11] and Tvergaard and Hutchinson [12, 13]. A key concept in this type of model is the use of two parameters to describe the fracture properties of the adhesive layer. Under LEFM conditions, only the intrinsic toughness of the adhesive layer, Γ_{10} , is required for the pure opening mode of fracture. With extensive plastic deformation, this single parameter does not result in a unique description of the fracture process; a second parameter, the peak stress supported by the adhesive layer, $\hat{\sigma}$, is needed. A number of mode-I geometries have been analyzed, including the wedge test [7, 14], T-peel test [7], and the

peel test [8], demonstrating how these two parameters provide a quantitative basis for predicting fracture. Using this cohesive-zone approach to investigate the fracture parameters of a wedge specimen made with a 0.25 mm thick commercial adhesive (XD4600 from Ciba Specialty Products), values of $\Gamma_{I_0} = 1.4 \pm 0.2 \text{ kJ/m}^2$ and $\hat{\sigma} = 100 \text{ MPa}$ were found for cohesive failure of the joint [14]. These values were confirmed using other thin-adherend geometries such as the T-peel and peel tests [7, 8]. It should be emphasized that the value of Γ_{I_0} obtained when the adherends deformed plastically is very different from published values of about 2.8 kJ/m^2 obtained for cohesive failure of joints made using the same adhesive but tested under LEFM conditions [15]. The apparent discrepancy between these two sets of data formed the impetus for the work presented here. However, it should be noted that there is, in fact, no *a priori* reason to assume that the toughness of an adhesive layer does not change when the adherends undergo substantially different modes of deformation. The toughness is dictated by the details of the local stresses acting at the crack tip, which may, in turn, depend on the deformation of the adherends. While the development of LEFM has established a framework by which one can ensure that the local stresses at the crack tip (and, hence, the toughness) are independent of the overall geometry, the local stresses are not expected to remain constant if the conditions for LEFM are violated.

2. EXPERIMENTAL

The toughness of a commercial adhesive (XD4600 from Ciba Specialty Products) was determined using double-cantilever beam (DCB) and tapered double-cantilever beam (TDCB) geometries. The adherends were fabricated from 6061-T6 aluminum with a height, h , for each adherend sufficient to prevent plastic deformation [10]. For the DCB specimens, this height was 36 mm. Adherends for the TDCB specimens were machined with a straight taper so that the quantity

$$m = \frac{3a^2}{h^3} + \frac{1}{h} \approx 725 \text{ m}^{-1} \quad (1)$$

where a is the current crack length and h is the specimen height at the crack tip. The bonding surfaces of the adherends were machined smooth and washed with acetone. A pre-crack was created by placing a strip of Teflon[®] tape across the bonding surfaces of both adherends before applying the adhesive. Uniform glass beads were randomly sprinkled onto the adhesive to maintain a constant bondline thickness of 0.25 mm. The specimens were then clamped and cured at 180°C for 1 hour. This was followed by air cooling to room temperature, and any excess adhesive along the edges of the specimen was removed using a rotating steel brush. The specimens were loaded in a screw-driven mechanical testing machine using displacement control at a rate of 1 mm/min. The strain was measured using an extensometer between the loading points, and a camera was used to measure crack growth and to observe the deformation of the adhesive layer along the side of the specimen. Several tests were conducted for each geometry, and sample load–strain curves are shown in Figures 1 and 2 for the DCB and TDCB specimens, respectively.

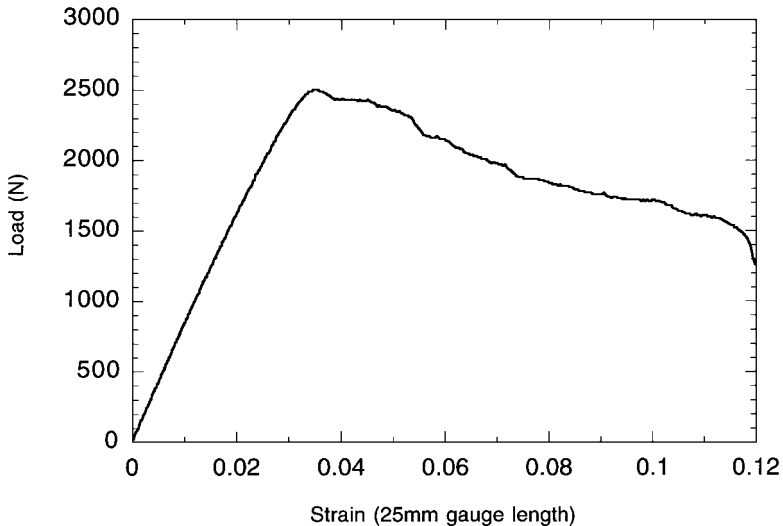


FIGURE 1 An example of an experimental load–strain curve for a DCB specimen (Al 6061 -T6 adherends) fabricated with a 0.25 mm thick layer of XD4600. For this specimen, $h = 34.0$ mm, $a = 73.0$ mm, $b = 9.53$ mm. This specimen was tested at a displacement rate of 1 mm/min.

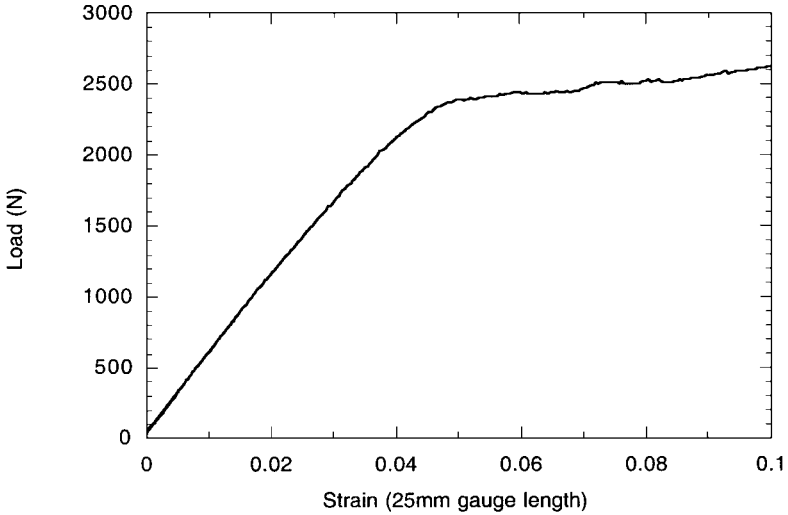


FIGURE 2 An example of a load–strain curve for a TDCB specimen (Al 6061-T6 adherends) fabricated with a 0.25 mm bondline of XD4600. The geometrical parameter m (defined in Eq. (1)) for this specimen was 697m^{-1} at the initial crack tip. This specimen was tested at a displacement rate of 1 mm/min.

The applied energy-release rate, \mathcal{G}_∞ , for a DCB geometry with isotropic, elastic adherends has been calculated numerically [16, 17]. An empirical fit to these results is given by

$$\mathcal{G}_\infty = \frac{12P^2a^2}{Eb^2h^3} \left[1 + 0.677 \frac{h}{a} \right]^2 \quad (2)$$

where P is the applied load, a is the distance from the applied load to the crack tip, h is the height of each adherend (36 mm), b is the specimen width (9.5 mm), and E is the Young's modulus of the adherends (69 GPa). Since the crack was observed to begin propagating at the peak load, this load can be used in Eq. (2) to obtain a value of the toughness. An approximate result for the applied energy-release rate of the TDCB geometry is given by [9]

$$\mathcal{G}_\infty = \frac{4P^2m}{Eb^2}. \quad (3)$$

A value for the toughness can be obtained from this equation by using the load at the beginning of the plateau in Figure 2. Assuming

that these equations are appropriate, the data of Figures 1 and 2 indicate that the mode-I toughness for cohesive failure of the XD4600 is $2.8 \pm 0.4 \text{ kJ/m}^2$. This is significantly higher than the value of $\Gamma_{I0} = 1.4 \pm 0.2 \text{ kJ/m}^2$ obtained when the adherends deform plastically [14].

3. DISCUSSION

Two points on the load-strain curves shown in Figures 1 and 2 are of special interest. The first is the point at which the crack begins to grow in a macroscopic fashion. This corresponds to the maximum load for the DCB specimens and to the onset of the approximate plateau region for the TDCB specimens. The second point of interest is the end of the linear response for each specimen. Both figures show an initial linear region followed by a region of nonlinear behavior before the onset of crack growth. As discussed below, it is this non-linear behavior that is directly responsible for the higher values of toughness being obtained from the elastic specimens than from the plastically-deforming specimens.

Experimental observations indicated that the deviation from linearity was associated with the formation of voids in the adhesive ahead of the crack tip (perhaps nucleated by the presence of brittle inorganic filler particles [18]). Typically, small voids were visible at the edge of the adhesive layer between 5 and 25 seconds after the onset of the non-linearity. The initial damage zone appeared to extend about 3 to 5 mm ahead of the crack tip, but then grew as the load increased and reached a maximum length of 25–30 mm just before the crack began to propagate. Void nucleation and growth continued throughout the damage zone as the load was increased, so that eventually the surfaces of the adherends were bridged by ligaments of adhesive. Macroscopic crack growth occurred by the coalescence of the damage with the crack when the crack-tip opening displacement was about 0.6 mm. This is illustrated in Figure 3 which shows a side view of a DCB specimen about 5 mm ahead of the initial crack tip a few seconds after the peak load has been reached. Subsequent crack growth occurred with a damage zone of approximately constant length being maintained ahead of the crack. The energy-release rate at which the

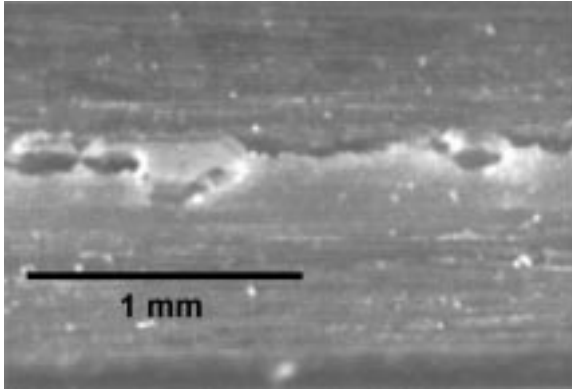


FIGURE 3 View of adhesive bridging ligaments approximately 5–10 mm ahead of a crack tip in a DCB specimen (Al 6061-T6 adherends) fabricated with a 0.25 mm thick layer of XD4600. The picture was taken a few seconds after the peak load had been reached, and the first ligaments at the crack tip had broken.

nonlinear deformation began was determined from Eqs. (1) and (3) to be about $1.1 \pm 0.3 \text{ kJ/m}^2$. It should be noted that this is lower than the value of the critical energy-release rate for crack propagation under conditions when the adherends deform plastically [14].

The difference between the behavior of the elastic joints, described above, and that observed for the plastically-deforming joints [14] suggests that there is a significant difference in the stress states of the two systems. In the elastic configuration, the constraint may be sufficiently high to cause cavitation before fracture and, hence, to allow a damage zone to develop. To explore this possibility, 2-D finite-element calculations were performed (using ABAQUS v.5.8) to investigate the stresses in the different geometries. Continuum elements¹ with constitutive properties determined from uniaxial tests were used for the adherends and for the adhesive layer. Specifically, the behavior of the 0.25 mm thick adhesive layer was taken to be time-independent, with a yield stress of 38 MPa, a Young's modulus of 3.6 GPa, and a Poisson's ratio of 0.35. The uniaxial stress-strain curve after yield was modeled by a piece-wise representation of the curve

¹ Simulations of geometries with elastic adherends used plane-stress elements for the adherends and plane-strain elements for the adhesive. Simulations of geometries with plastic adherends used plane-strain elements for both.

given in Ref. [14], and a pressure-insensitive von Mises yield criterion was assumed. The appropriate experimental geometry was modeled for each test (with a 1 mm thick specimen for the simulation of the wedge test of Ref. [14]).

The opening stress ahead of the crack tip is plotted in Figure 4 for both the elastic and plastic geometries. Calculations for the elastic adherends were done for an energy-release rate approximately corresponding to the onset of damage nucleation (1.1 kJ/m^2). The plastic calculations were done for an energy-release rate approximately corresponding to the onset of crack growth in that case (1.4 kJ/m^2) [14]. Previous work on stress distributions by He *et al.* [19] and Yan and Mai [20] predicted a similar distribution for the elastic configuration. The peak stress is several times the uniaxial yield strength of the adhesive and occurs at a location a few bond-line thicknesses ahead of the crack. In contrast, as also shown by Kafkalidis *et al.* [14], the results for the plastically-deforming wedge tests show a much smaller level of stress in the adhesive, even at the larger values of energy-release rate. For example, with the particular

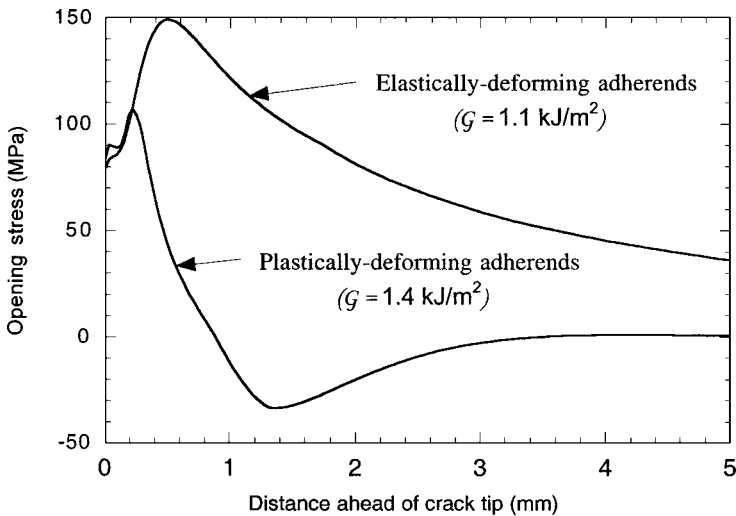


FIGURE 4 A comparison of the opening stress distributions in a plastically-deforming wedge-loaded joint and an elastically-deforming DCB joint. The thickness of the adhesive layer (XD4600) in both cases is 0.25 mm. The thickness for the adherends is 36 mm for the elastic DCB joint and 1 mm for the wedge-loaded joint.

conditions examined here, the peak stress in the wedge specimen at fracture is predicted to be only 105 MPa, whereas it is predicted to be approximately 150 MPa at the lower level of energy-release rate corresponding to damage nucleation with the elastic adherends. This suggests that the critical energy-release rate for fracture is reached with the plastically-deforming specimens before the constrained stress in the adhesive reaches a sufficient level for damage nucleation. This allows the crack to propagate in a continuous fashion from the tip. Conversely, damage occurs in the elastic specimens before fracture, reducing the local stress in the adhesive and allowing a damage zone to develop.

Nucleation of damage changes the deformation and fracture mechanisms of the adhesive layer, and affects the behavior of the joint. While damage nucleation cannot be expected always to result in a higher energy-release rate being achieved before fracture, in this particular system damage nucleation did appear to be beneficial. In general, the effect of a damage zone can be considered from two equally valid perspectives [21]. First, as shown in Figure 5, the damage zone may be modeled as a bridging zone behind the tip of a somewhat

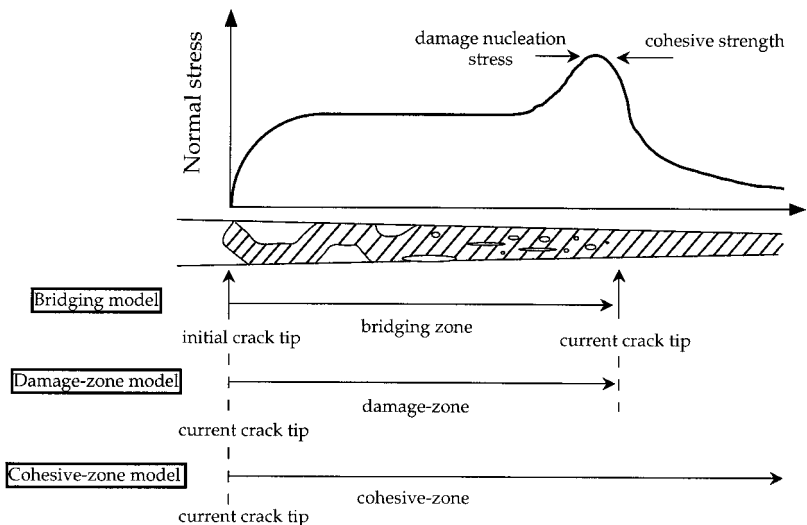


FIGURE 5 A schematic illustration of how the same events at a crack tip can be viewed either as a bridging-zone, a damage zone or a cohesive zone.

longer crack. Damage formation then corresponds to an extension of the crack with bridging. This leads to extrinsic toughening and R-curve behavior as the bridging (damage) zone increases in length [22]. A clear example of R-curve behavior caused by damage in an adhesive joint is given by Papini *et al.* [23]. It should be noted that crack advance (*i.e.*, damage nucleation) occurs when the energy-release rate at the crack tip (*i.e.*, the end of the damage zone) equals the intrinsic toughness of the material. Viewed from this perspective, it can be seen that whether damage nucleation is considered to be beneficial or not depends on whether the loss of intrinsic toughness caused by the onset of damage is out-weighed by the extrinsic toughening associated with bridging. The fact that an R-curve is noted in conjunction with damage, as in Ref. [23], does not necessarily mean that the damage is beneficial. The steady-state toughness needs to be compared with the intrinsic toughness of the adhesive layer without damage to determine whether damage nucleation is actually a toughening mechanism or an embrittling mechanism.

The second perspective of a damage zone is provided by cohesive-zone models of fracture [11 – 13]. In these models, the crack surfaces are held together by a characteristic traction-separation law, and crack advance occurs when the cohesive tractions at the crack tip drop to zero causing the crack surfaces to separate. The intrinsic toughness, Γ_{10} , of the adhesive layer is given by the area under the traction-separation curve. The effect of introducing damage can be viewed as increasing the size of the cohesive zone, and the deformation of the damage zone becomes an integral part of the traction-separation law of the cohesive zone (Fig. 5). In general, nucleation of damage will truncate the peak cohesive stress that the adhesive layer can support. If this occurs without any increase in the maximum strain that the adhesive layer can support, then the toughness is decreased by the introduction of damage. If, however, damage sufficiently increases the critical displacement for final separation of the adhesive layer, then the toughness of the system may be enhanced by damage. This is illustrated schematically in Figure 6. In conclusion, while damage nucleation can be viewed either from a bridging-zone or cohesive-zone perspective, whether damage nucleation results in toughening or embrittling depends on how the tractions and displacements across the adhesive layer are affected by the presence of the damage.

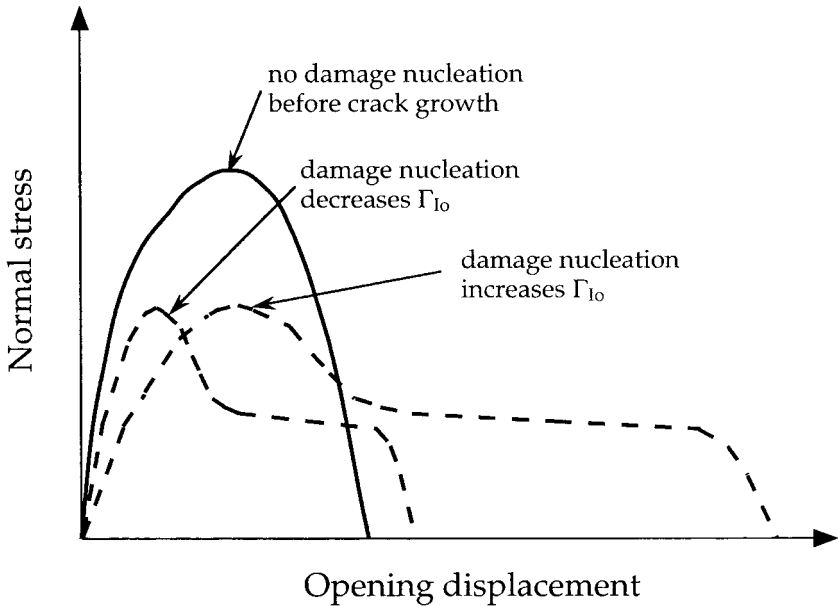


FIGURE 6 Schematic illustration of the cohesive stresses in a damage zone, illustrating when damage is beneficial or detrimental to the toughness of an adhesive system.

A large-scale damage (or bridging or cohesive) zone is responsible for the nonlinear deformation observed in Figures 1 and 2. Under these conditions, the LEFM results of Eqs. (2) and (3) are not appropriate for evaluating the toughness of the system [24], and a cohesive-zone model can be used to determine the fracture parameters. Using the trapezoidal traction-separation law shown in Figure 7,² normalized load-displacement curves for a DCB specimen are shown in Figure 8. Of particular note is that, for a fixed value of Γ_{I_0} , the maximum load supported by the specimen decreases as the cohesive strength, $\hat{\sigma}$, decreases. A toughness determined by using the maximum load in Eq. (2) would then give an underestimate [24]. This is further illustrated by Figure 9 which shows how the maximum load varies as a function of both the crack length and the cohesive strength. It can be

²The shape of the traction-separation law is not important, the essential features are captured by the cohesive strength, $\hat{\sigma}$, and the intrinsic toughness of the adhesive layer, Γ_{I_0} , (the area under the traction-separation curve).

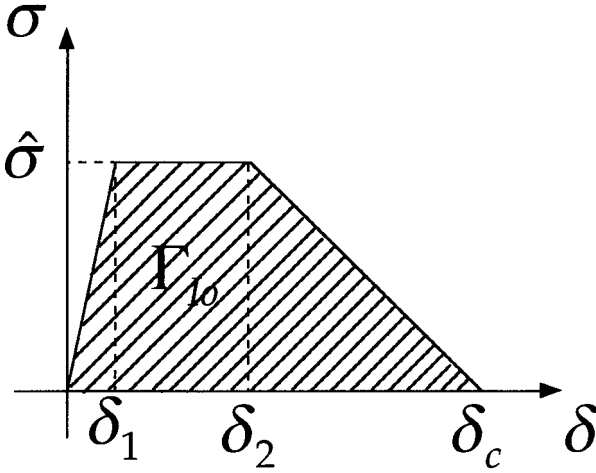


FIGURE 7 The traction-separation law used to model the response of the adhesive layer.

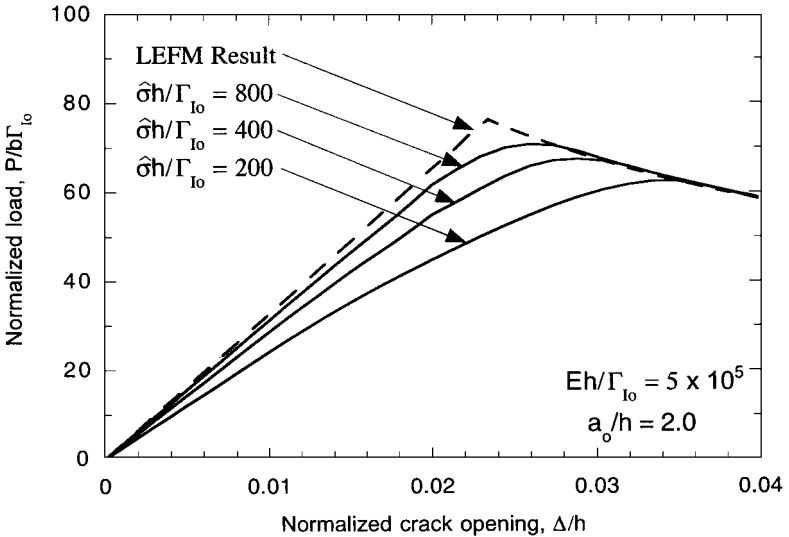


FIGURE 8 Non-dimensional plot of the load-displacement curves for a DCB specimen with different values of the fracture parameters.

seen that use of Eq. (2) is appropriate only when the initial crack length is very long or when the cohesive strength is large.

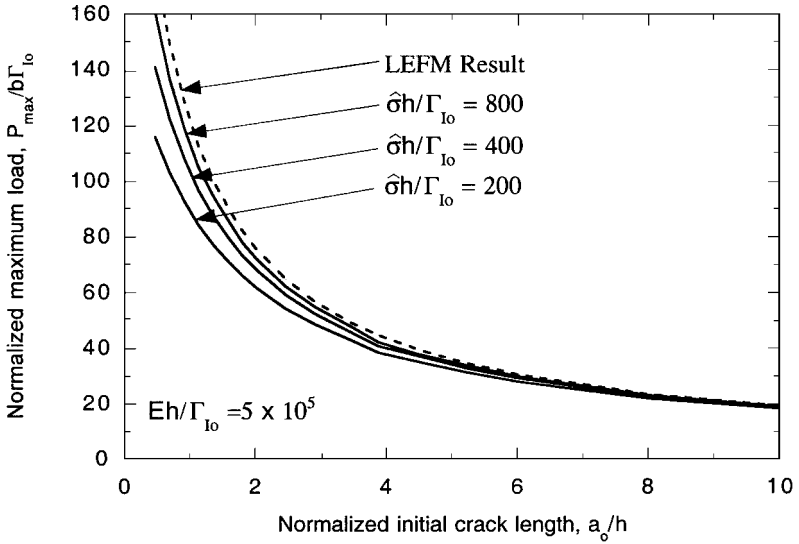


FIGURE 9 Non-dimensional plot of the peak load predicted from cohesive zone models showing the effect of the cohesive strength and geometry.

The approach of Williams [24], in which the cohesive zone is regarded as providing an effective increase in the crack length, provides a nice basis for empirical fits to the numerical results discussed above. It will be noted from Figure 8 that, for a fully-developed cohesive zone, the predicted loads coincide with those predicted by LEFM for longer cracks. In other words, it may be possible to determine an effective crack length (that will depend on $\hat{\sigma}h/\Gamma_{I_0}$) in the presence of a cohesive zone which can be used in Eq. (2) to determine the energy-release rate. In order to investigate this possibility, it is first noted that the results of finite-element calculations for the compliance of a linear-elastic double-cantilever beam geometry can be described by an empirical fit

$$\frac{\Delta}{h} = \frac{8P}{Ebh} \left(\frac{a}{h} + 0.677 \right)^3 \quad (4)$$

where Δ is the total opening at the crack mouth in response to an applied load P . This equation is accurate to within about 10% if $a/h = 1$, and rapidly becomes more accurate at larger crack lengths. It is found empirically that Eq. (4) reasonably describes the compliance of

the geometries with a cohesive zone shown in Figure 8 using an effective crack length of

$$\frac{a_{\text{effective}}}{h} = \frac{a}{h} + 120 \frac{\Gamma_{I0}}{\hat{\sigma}h} \quad (5)$$

Furthermore, if this effective crack length is used in Eq. (2) with the energy-release rate set to Γ_{I0} , the load required for crack propagation appears to be predicted fairly accurately. This provides a basis for estimating the cohesive-zone parameters from DCB results without resorting to numerical calculations. If the load and effective compliance are determined at any point on the load–displacement curve at the point of crack growth (or when the crack is propagating), and the nominal crack length is known, then the use of Eqs. (2) (set equal to Γ_{I0}), (4) and (5) and provide two equations from which to estimate the two unknowns, Γ_{I0} and $\hat{\sigma}$. While Eq. (5) was specifically developed for a value of $Eh/\Gamma_{I0} = 5 \times 10^5$, the relationship is not expected to be very sensitive to small changes in this parameter.

In the light of the results of the previous paragraph, it is of interest to determine a corrected value of the toughness for the particular system studied here. This was done by comparing the numerical predictions with the experimental observations for the shape of the load-displacement curve and the peak load. This indicates that the two fracture parameters are $\hat{\sigma} = 35 \pm 3$ MPa, and $\Gamma_{I0} = 3.4 \pm 0.5$ kJ/m². It should be noted that, owing to the relatively large scale of the damage zone, the actual toughness of this system is significantly higher than was originally deduced from a simple LEFM analysis of the experimental data. Figure 10 shows how the numerical results compare with the experimental data.

The magnitude of $\hat{\sigma}$ can be confirmed by viewing it as a bridging stress, and comparing the compliance from continuum finite-element calculations, in which the damage zone has been replaced by a region of constant stress, with the experimentally-measured value. When viewed as a bridging zone, the effect of damage is to provide an R-curve where the toughness increases from an intrinsic value of 1.1 kJ/m² to a fully-toughened value of 3.4 kJ/m² after about 25 mm of crack growth. The extrinsic toughening attributed to bridging is, therefore, about 2.3 kJ/m², with a bridging stress of 35 MPa. An estimate for the extrinsic toughness can be obtained from the product of the bridging

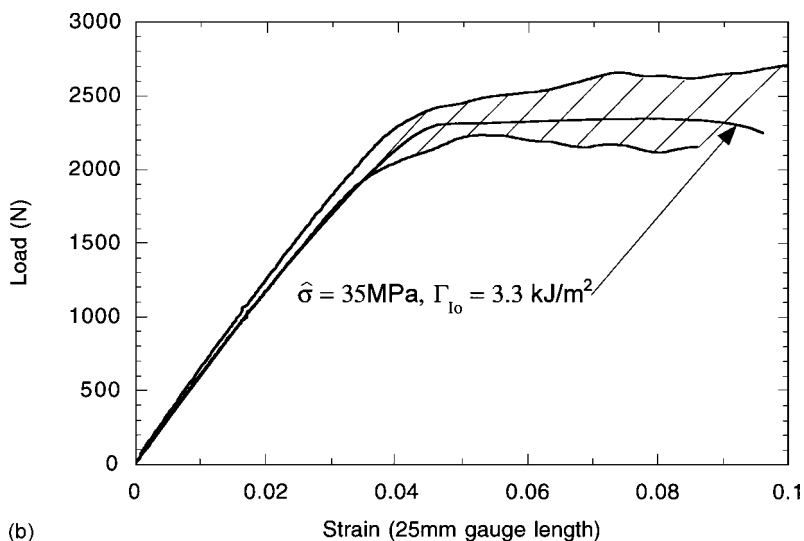
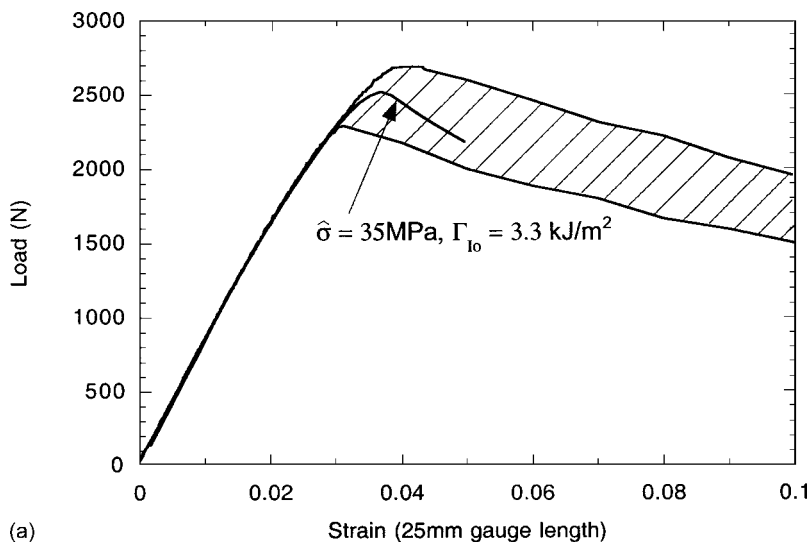


FIGURE 10 A comparison between the results of a cohesive-zone model (with $\hat{\sigma} = 35 \text{ MPa}$, and $\Gamma_o = 3.3 \text{ kJ/m}^2$) for the fracture of (a) a DCB specimen and (b) a TDCB specimen and experimental observations for both geometries. The shaded region shows the range of experimental results.

stress and the failure displacement of the bridging ligaments [22]. Since δ_c was observed to be 0.6 ± 0.1 mm, this approximation results in a predicted value for the extrinsic toughening of about 2.1 ± 0.4 kJ/m², which illustrates a consistency between the deduced values of the fracture parameters.

4. CONCLUSIONS

The intrinsic toughness of an adhesive layer is not constant. It depends on the constraint exerted on it by the surrounding adherends. If a change in the constraint alters the deformation mechanisms of the adhesive layer, then the measured toughness of a joint may change. In the case studied here, the relatively low constraint associated with plastic deformation of the adherends resulted in the adhesive layer fracturing in a continuous fashion from the crack tip. However, with elastic adherends, the constraint was elevated to such an extent that void nucleation and growth occurred before macroscopic crack propagation. The large-scale bridging that this induced resulted in a substantially enhanced level of toughness at steady state (even though the level of the applied energy-release rate at which damage was nucleated was lower than the intrinsic toughness appropriate for the plastically-deforming adherends). When such large-scale bridging or cohesive zones develop, the magnitude of both the cohesive tractions across the adhesive layer and the intrinsic toughness need to be determined numerically when analyzing the properties of an adhesive joint. In the particular system studied here, the large-scale bridging resulted in a maximum toughness of about 3.4 kJ/m² with the elastic adherends, as opposed to only about 1.4 kJ/m² when the adherends deformed in a plastic fashion.

Observations of the opening at the crack tip indicated that these values of toughness were consistent with the peak cohesive stresses deduced from numerical simulations with a cohesive zone. The results suggest that when designing tough adhesives, the use of a weak phase to introduce damage is a viable option. However, introduction of damage alone does not guarantee an enhanced toughness, and its effect must be analyzed carefully from a micro-mechanics viewpoint

(either in terms of a bridging or of a cohesive zone) to determine whether it is beneficial.

Acknowledgements

The authors would like to thank Dr. Q. D. Yang, Dr. S. M. Ward, Dr. J. Hill and Mr. M. S. Kafkalidis for their assistance in the development of this work. Support for M. N. Cavalli was provided through a National Science Foundation graduate fellowship. This work was partially supported by NSF grant # CMS 9624452 and Ford Motor Company.

References

- [1] Wagner, D. A., Cunningham, C. M. and Debolt, M. A., "Weld Bonded Joint Design: Pickup Box Case Study", *Proc. of Int. Body Eng. Conf.* pp. 123–128 (1993).
- [2] Kinloch, A. J., *Adhesion and Adhesives: Science and Technology* (Chapman and Hall, London, 1987).
- [3] Gent, A. N. and Kinloch, A. J., "Adhesion of Viscoelastic Materials to Rigid Substrates – 3. Energy Criterion for Failure", *J. Polymer Science* **9**, 659–668 (1971).
- [4] Gledhill, R. A., Kinloch, A. J., Yomani, S. and Young, R. S., "Relationship Between Mechanical Properties of and Crack Propagation in Epoxy Resin Adhesives", *Polymer* **19**, 574–582 (1978).
- [5] Kim, K.-S. and Kim, J., "Elasto-Plastic Analysis of the Peel Test for Thin Film Adhesion", *J. Eng. Mat. and Tech.* **110**, 266–273 (1988).
- [6] Kim, K.-S. and Aravas, N., "Elastoplastic Analysis of the Peel Test", *Int. J. Solids and Structures* **24**, 417–435 (1988).
- [7] Yang, Q. D., Thouless, M. D. and Ward, S. M., "Numerical Simulations of Adhesively Bonded Beams Failing with Extensive Plastic Deformation", *J. Mech. and Phys. of Solids* **47**, 1337–1353 (1999).
- [8] Yang, Q. D., Thouless, M. D. and Ward, S. M., "Analysis of the Symmetrical 90° – Peel Test with Extensive Plastic Deformation", *J. Adhesion* **72**, 115–132 (2000).
- [9] Yang, Q. D., Thouless, M. D., "Mixed-mode Fracture Analysis of Plastically-Deforming Adhesive Joints", submitted to *Int. J. Fract* (2000).
- [10] "Standard Test Method for Fracture Strength in Cleavage of Adhesives in Bonded Joints", Standard D 3433–93, *ASTM* (1999).
- [11] Needleman, A., "A Continuum Model for Void Nucleation by Inclusion Debonding", *J. Applied Mech.* **54**, 525–531 (1987).
- [12] Tvergaard, V. and Hutchinson, J. W., "The Relation Between Crack Growth Resistance and Fracture Process Parameters in Elastic-Plastic Solids", *J. Mech. and Phys. of Solids* **40**, 1377–1397 (1992).
- [13] Tvergaard, V. and Hutchinson, J. W., "On the Toughness of Ductile Adhesive Joints", *J. Mech. and Phys. of Solids* **44**, 789–800 (1996).
- [14] Kafkalidis, M. S., Thouless, M. D., Yang, Q. D. and Ward, S. M., "Deformation and Fracture of an Adhesive Layer Constrained by Plastically-Deforming Adherends", *Int. J. of Adhesion Sci. and Tech.* in press (2000).

- [15] Kinloch, A. J., Blackman, B. R. K., Taylor, A. C. and Wang, Y., "The Failure of Adhesively-Bonded Joints Under High Rates of Deformation", *Proceedings of the Euradh '96 Conference*, Institute of Materials, London, UK, pp. 467–472 (1996).
- [16] Suo, Z., Bao, G., Fan, B. and Wang, T. C., "Orthotropy Rescaling and Implications for Fracture in Composites", *Int. J. Solids and Structures* **28**, 235–248 (1991).
- [17] Wiederhorn, S. M., Shorb, A. M. and Moses, R. L., "Critical Analysis of the Theory of the Double Cantilever Method of Measuring Fracture-Surface Energies", *J. Applied Phys.* **39**, 1569–1572 (1968).
- [18] Bysh, I. N., Crocombe, A. D. and Smith, P. A., "Determining the Effective Material Properties of Damaged Particle Filled Adhesives", *J. Adhesion* **58**, 205–226 (1996).
- [19] He, M. Y., Evans, A. G. and Hutchinson, J. W., "Interface Cracking Phenomena in Constrained Metal Layers", *Acta Mater.* **44**, 2963–2971 (1996).
- [20] Yan, C. and Mai, Y. W., "Effect of Constraint on Void Growth Near a Blunt Crack Tip", *Int. J. Fracture* **92**, 287–304 (1998).
- [21] Thouless, M. D., "Bridging and Damage Zones in Crack Growth", *J. Am. Ceram. Soc.* **71**, 408–413 (1988).
- [22] Budiansky, B., "Micromechanics II", *Proc. of 10th U.S. Nat. Conf. of Applied Mech.* pp. 25–32 (1986).
- [23] Papini, M., Fernlund, G. and Spelt, J. K. "Effect of Crack Growth Mechanism on the Prediction of Fracture Load of Adhesive Joints", *Comp. Sci. and Tech.* **52**, 561–570 (1994).
- [24] Williams, J. G., "Fracture in adhesive joints – the beam on elastic foundation model", *Proceedings of ASME International Mechanical Congress and Expositions* pp. 1112–1117 (1995).